Journal of Advanced Research in Fluid Mechanics and Thermal Sciences 105, Issue 2 (2023) 51-67

Journal of Advanced Research in Fluid Mechanics and Thermal Sciences

Journal homepage:
https://semarakilmu.com.my/journals/index.php/fluid_mechanics_thermal_sciences/index
ISSN: 2289-7879

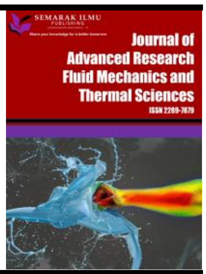

Hall Current and Thermal Radiation Effects on MHD Casson Nanofluid Flow Past in The Presence of Heat Source/Sink, Brownian Motion and Thermophoresis

Deepthi Varagani Venkata Lakshmi[1,*], Srinivasa Raju Rallabandi[2]

[1] Department of Mathematics, CVR College of Engineering, Hyderabad-501506, Telangana State, India
[2] Department of Mathematics, GITAM University (Deemed to be University), Hyderabad campus, Rudraram, Sanga Reddy (Dt)-502329, Telangana State, India

ARTICLE INFO

Article history:
Received 29 December 2022
Received in revised form 5 April 2023
Accepted 12 April 2023
Available online 28 April 2023

Keywords:
Hall effect; thermal radiation; Casson fluid; heat source/sink

ABSTRACT

The effect of Hall current and thermal radiation on the MHD flow of an electrically conducting Casson nanofluid across a constantly extending surface in the presence of Heat source/sink, Brownian motion and Thermophoresis has been analyzed and investigated. Vertical application of a transverse magnetic field, with the premise that the Reynolds number is relatively low. The appropriate similarity transformations are used to convert the controlling partial differential equations into non-linear ordinary differential equations. The shooting technique generates numerical solutions for the dimensionless velocity, temperature, and nanoparticle concentration. These three variables are all taken into consideration. The findings are bolstered further by the outcomes acquired via MATLAB's built-in functions. Using graphs, the discussion will focus on the effects that the hall current parameter, thermal radiation parameter, Brownian motion parameter, thermophoresis parameter, and magnetic parameter have on the velocities, concentrations, and temperatures. To get insight into the internal behavior of the emerging parameters, a numerical calculation of the skin friction coefficient along the x and z axes, the local Nusselt number, and the Sherwood number are all performed.

1. Introduction

Casson fluid is a non-Newtonian (visco-inelastic) fluid with yield stress representing blood flow in narrow arteries. When blood flows from larger diameter arteries at high shear rates, it shows Newtonian character. But it exhibits non-Newtonian behavior when it flows through small diameter arteries at low shear rates (Rathod and Tanveer [1]). Also, blood viscosity increases at low shear rates as the red blood cells aggregate into the Rouleaux form. This non-Newtonian behavior of blood flow presents a flattened parabolic velocity profile rather than the parabolic velocity profile of a Newtonian fluid. The non-Newtonian characteristic is due to yield stress. The yield stress values for normal human blood are between 0.01 and 0.06 dyn/cm^2 (Krishnan *et al.,* [2]). The blood flow in

* *Corresponding author.*
E-mail address: deepthisri.cute@gmail.com

https://doi.org/10.37934/arfmts.105.2.5167

narrow arteries at low shear rates represents Casson fluid characteristics (Blair [3,4]). Further, Li *et al.,* [5] have studied Effects of activation energy and chemical reaction on unsteady MHD dissipative Darcy–Forchheimer squeezed flow of Casson fluid over horizontal channel. A very recently Kumar *et al.,* [6] have discussed Numerical analysis of magnetohydrodynamics Casson nanofluid flow with activation energy, Hall current and thermal radiation. Umair Khan *et al.,* [7] have discussed An exact solution of a Casson fluid flow induced by dust particles with hybrid nanofluid over a stretching sheet subject to Lorentz forces. Raza *et al.,* [8] have studied the flow of magnetised convective Casson liquid via a porous channel with shrinking and stationary walls. Sohail *et al.,* [9] have possessed Contribution of joule heating and viscous dissipation on three dimensional flow of Casson model comprising temperature dependent conductance utilizing shooting method. Oudina *et al.,* [10] have expressed Hydromagnetic flow of magnetite–water nanofluid utilizing adapted Buongiorno model. Raghunath and Obulesu [11] have studied Unsteady MHD oscillatory Casson fluid flow past an inclined vertical porous plate in a chemical reaction with heat absorption and Soret effects. Raghunath *et al.,* [12] studied the Investigation of MHD Casson fluid flow past a vertical porous plate under thermal diffusion and chemical reaction.

The idea of nanofluid was first introduced by Choi [13] in 1995. The homogeneous mixture of very small particles of size 10−9m and base fluid is called nanofluid. Usually, Al, Cu, Ag, TiO_2, Al_2O_3, etc., are used as nanoparticles with base fluids like oil, ethylene glycol, water, etc. While using the nanofluids, the maximum possible thermal properties are targeted to achieve the least feasible concentration by systematic dispersion and substantial suspension of nanoparticles in the base fluids [14,15]. These fluids are fit for enhancing the thermophysical properties, for example, thermal diffusivity, convective heat transfer coefficient, viscosity, and thermal conductivity, when compared with those of the base liquids like ethylene, tri-ethylene glucose, water or other coolants, polymer solutions, and biofluids as expatiated by Choi [13], and Wong and Leon [16]. These fluids possess distinguished physical and chemical properties, can easily pass through the microchannels and capillaries, and don't block the flow. Fuel cells, hybrid-powered instruments, automotive, food handling industry, and refrigeration are pertinent examples of nanofluids. Buongiorno [17] considered the Brownian diffusion and thermophoresis slip mechanism for the relative velocity of the base fluid and nanoparticles. He proposed a mathematical model involving thermophoresis and the Brownian motion effects to examine the thermal effects of the host fluid. Later on, Mebarek-Oudina [18] has expressed convective heat transfer of Titania nanofluids of different base fluids in cylindrical annulus with discrete heat source. Shafiq *et al.,* [19] have possessed Sensitivity analysis for Walters-B nanoliquid flow over a radiative Riga surface by RSM. Mebarek-Oudina and Chabani [20] reviewed the review on Nano-Fluids Applications and Heat Transfer Enhancement Techniques in Different Enclosures. Dharmaiah *et al.,* [21] have expressed Nuclear reactor application on Jeffrey fluid flow with Falkner-skan factor, Brownian and thermophoresis, non linear thermal radiation impacts past a wedge. Chabani *et al.,* [22] have studied Ismail, Numerical analysis of magnetic hybrid Nano-fluid natural convective flow in an adjusted porous trapezoidal enclosure. In another article, Nazir *et al.,* [23] have studied Finite element simulations of hybrid nano-Carreau Yasuda fluid with hall and ion slip forces over rotating heated porous cone. Rabeeah Raza *et al.,* [24] have discussed Exploration of temperature-dependent thermal conductivity and diffusion coefficient for thermal and mass transportation in sutterby nanofluid model over a stretching cylinder. Sohail *et al.,* [25] have analyzed Computational exploration for radiative flow of Sutterby nanofluid with variable temperature-dependent thermal conductivity and diffusion coefficient. Naseem *et al.,* [26] have reviewed Contribution of Dufour and Soret effects on hydromagnetized material comprising temperature-dependent thermal conductivity. Wang *et al.,* [27] have expressed Galerkin strategy for tri-hybridized mixture in ethylene glycol comprising variable diffusion and thermal conductivity using non-Fourier's theory. Algehyne *et al.,* [28] have possessed Investigation of thermal performance of Maxwell hybrid nanofluid boundary value problem in vertical porous surface via finite element approach. Sohail *et al.,* [29] have investigated Theoretical and numerical investigation of entropy for the variable thermophysical characteristics of couple stress material, Applications to optimization. They considered five different types of nanoparticles: aluminum oxide, titanium oxide, copper oxide, iron oxide, and graphene oxide, with three base fluids: kerosene oil, water, and engine oil.

Hall current is most prominent in the absolute value and orientation of the current density and, thereby, the magnetic force term. Under the effects of Hall currents, the convective flow problem with the magnetic field is significant because of engineering uses in electric transformers, transmission lines, refrigeration coils, power generators, MHD accelerators, nanotechnological processing, nuclear energy systems exploiting liquid metals, blood flow control, and heating elements. In the case of a magnetic field of high strength and low density in the gas, the investigation of magnetohydrodynamic flows with Hall current has the best utilization in studying Hall accelerators and flight Magnetohydrodynamics. The Hall Effect plays an important role when the Hall parameter is high. Hall parameter is the ratio of electron cyclotron frequency to atom-electron collision frequency. Maatoug *et al.,* [30] have studied Variable chemical species and thermo-diffusion Darcy–Forchheimer squeezed flow of Jeffrey nanofluid in horizontal channel with viscous dissipation effects. Omar *et al.,* [31] have analyzed Hall Current and Soret Effects on Unsteady MHD Rotating Flow of Second-Grade Fluid through Porous Media under the Influences of Thermal Radiation and Chemical Reactions. Deepthi *et al.,* [32] have discussed Recent Development of Heat and Mass Transport in the Presence of Hall, Ion Slip and Thermo Diffusion in Radiative Second Grade Material: Application of Micromachines. Aruna *et al.,* [33] have possessed An unsteady MHD flow of a second-grade fluid passing through a porous medium in the presence of radiation absorption exhibits Hall and ion slip effects. One dimensional unsteady MHD micropolar fluid flow with the development of Hall current was analyzed by Islam *et al.,* [34]. The chemically reactive second grade via porous saturated space was investigated by Raghunath *et al.,* [35] using a perturbation technique. Raghunath *et al.,* [36] have investigated the effects of Soret, Rotation, Hall, and Ion Slip on the unsteady flow of a Jeffrey fluid through a porous medium. Raghunath and Mohanaramana [37] have researched Hall, Soret, and rotational effects on unsteady MHD rotating flow of a second-grade fluid through a porous media in the presence of chemical reaction and aligned magnetic field.

Thermal radiation plays a vital role in dissipating heat from the surface. It has applications in manufacturing industries such as choppers, space vehicles, reliable equipment design, satellites, atomic furnaces, missiles, space technology, and procedures related to high temperatures. Dharmendra *et al.,* [38] analyzed thermal radiation and suction effects on MHD nanofluid boundary layer flow on a non-linear stretching sheet. Kothandapani and Prakash [39] observed peristaltic transport in a tapered asymmetric channel of a Williamson Nanofluid in the presence of thermal radiation. Sulochana *et al.,* [40] analyzed the effects of short and suction/blowing on the MHD stagnation point flow of a radiative Carreau nanofluid on a stretching surface. Kho *et al.,* [41] investigated the impact of radiation on MHD heat and mass transfer and Casson nanofluid flow on a porous stretching sheet. Zubair *et al.,* [42] have discussed Computational analysis of radiative Williamson hybrid nanofluid comprising variable thermal conductivity.

The study of heat generation/absorption parameter on the moving fluid is influential in sight of diverse physical problems. Uneven heat generation plays a crucial part in heat dissipation problems. With the accelerated development of electronic technology, efficient cooling of electronic equipment has evolved to cool various electronic equipment and is provided by separate transistors for mainframes and power supplies for telephone switches. The influence of heat generation/absorption plays a crucial role in the heat efficiency of base fluids. Its pertinence is seen in the heat discharge of nuclear fuel residues, food storage, the production of plastic and rubber sheets, the motion of fluids in fixed bed reactors, and much more. Recently, Raghunath *et al.,* [43] studied the Heat absorption effects on dissimilar flow geometries. Raghunath and Mohana Ramana [44] studied Soret and chemical reaction effects on heat and mass transfer in MHD flow of a Kuvshinski fluid through porous medium with aligned magnetic field and radiation. Raghunath *et al.,* [45] have possessed Chemical reaction with aligned magnetic field effects on unsteady MHD Kuvshinski fluid flow past an inclined porous plate in the presence of radiation and Soret effects. Obulesu *et al.,* [46] have investigated MHD heat and mass transfer steady flow of a convective fluid through a porous plate in the Presence of diffusion thermo and aligned magnetic field.

The study that Sureshkumar *et al.,* [47] did was the foundation for the current investigation, which is an extension of that work. In this research, we investigated the effects of Hall current and thermal radiation on an electrically conducting Casson nanofluid fluid flow past in a vertical direction in the presence of Heat source/sink, Brownian motion and Thermophoresis were presented. The governing partial nonlinear differential equations of flow, heat, and mass transfer are transformed into ordinary differential equations via a similarity transformation. This allows for a more straightforward analysis. After that, the issues are solved using numerical methods. The consequences of several non-dimensional regulating parameters on velocity, temperature, and concentration profiles are discussed, and the results are shown graphically. When specific conditions are satisfied, the present study's findings show an exceptionally high degree of unity with the findings of previous investigations.

2. Formulation of The Problem

Here, steady heat and mass transfer of an incompressible hydromagnetic nanofluid flow along a vertical stretching sheet coinciding with the plane $y = 0$, has been considered in the presence of the Hall current effects. By keeping the origin fixed, two opposite and equal forces are assumed to employ along the x-axis so that the sheet stretches linearly in both positive and negative direction (see Figure 1).

i. With the assumption that the Newtonian nanofluid be electrically conducting and heat generating/absorbing, a strong magnetic field has been imposed normal to the direction of flow.
ii. Moreover, no electric field has been assumed to apply and the frequency of atom-electron collision has also been considered high for the generation of Hall current effect [48].
iii. Due to the strong magnetic flux density B_0, the Hall current effect is taken into consideration, however the small magnetic Reynolds number is employed and the induced magnetic field is ignored.
iv. Hall current effect is strong enough to give rise to a force in the z−direction and a cross flow is induced in the same direction which causes a three dimensional flow. It is further assumed that there are no variations in the flow, heat and mass transfer in the z-direction.
v. This assumption can be achieved by taking the sheet of infinite width. Non-conducting plate is considered so that the generalized Ohm’s law [49] in the flow field.
vi. Brownian motion and thermophoresis effects are considered using the Buongiorno model for the nanofluid. Further, the effects of viscous dissipation and Joule heating are ignored.

The governing equations for Casson nanofluid along with continuity equation are followed by sureshkumar [47].

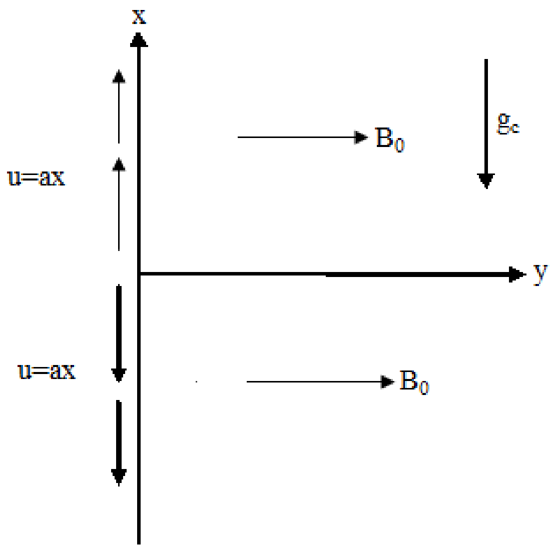

Fig. 1. Physical sketch and coordinate system

In light of the premises discussed earlier and the Boussinesq approach, the following is the arithmetical representation of the problem

$$\frac{\partial u}{\partial x}+\frac{\partial u}{\partial y}=0, \tag{1}$$

$$u\frac{\partial u}{\partial x}+v\frac{\partial u}{\partial y}=\nu\left(1+\frac{1}{\beta}\right)\frac{\partial^2 u}{\partial y^2}-\frac{\sigma B_0^2}{\rho\left(1+m^2\right)}\left(mw+u\right)+g_C\beta_T(T-T_\infty)+g_C\beta_C(C-C_\infty), \tag{2}$$

$$u\frac{\partial w}{\partial x}+v\frac{\partial w}{\partial y}=\nu\left(1+\frac{1}{\beta}\right)\frac{\partial^2 w}{\partial y^2}+\frac{\sigma B_0^2}{\rho\left(1+m^2\right)}\left(mu-w\right), \tag{3}$$

$$u\frac{\partial T}{\partial x}+v\frac{\partial T}{\partial y}=\frac{k}{\rho C_p}\frac{\partial^2 T}{\partial y^2}+\frac{Q_0}{\rho C_p}(T-T_\infty)+\tau\left(D_B\frac{\partial C}{\partial y}\frac{\partial T}{\partial y}+\frac{D_T}{T_\infty}\left(\frac{\partial T}{\partial y}\right)^2\right)-\frac{1}{\rho C_p}\frac{\partial q_r}{\partial y}, \tag{4}$$

$$u\frac{\partial C}{\partial x}+v\frac{\partial C}{\partial y}=D_B\frac{\partial^2 C}{\partial y^2}+\frac{D_T}{T_\infty}\frac{\partial^2 T}{\partial y^2}. \tag{5}$$

The associated boundary conditions for the PDEs that are in charge are as follows

$$\begin{aligned} &u=ax,\quad v=0,\quad w=0,\quad T=T_w,\quad C=C_w \quad &\text{at } y=0,\\ &u\to 0,\quad v\to 0,\quad w\to 0,\quad T\to T_\infty \quad C\to C_\infty \quad &\text{as } y\to\infty. \end{aligned} \tag{6}$$

The similarity conversion that was used so that the PDEs may be translated into dimensionless ODEs

$$\eta=\sqrt{\frac{a}{\nu}}y,\ \psi(x,y)=\sqrt{a\nu}x\,f(\eta),\ w=axg(\eta),\ \phi(\eta)=\frac{C-C_\infty}{C_w-C_\infty},\ \theta(\eta)=\frac{T-T_\infty}{T_w-T_\infty}. \tag{7}$$

Because an optically thick fluid also engages in self-absorption in contrast to emission, the Rosseland approximation may be used for the radiative heat flux vector qr. We can use the Rosseland approximation because the absorption coefficient is often dependent on the wavelength and is substantial. As a result, the value serves as the description of qr.

$$q_r=\frac{-4\sigma^*}{3k^*}\frac{\partial^2 T^4}{\partial y}, \tag{8}$$

In this equation, k^* denotes the Rosseland mean absorption co-efficient and σ_1 stands for the Stefan–Boltzmann constant.

Because we are functioning under the premise that the temperature fluctuations within the flow are not particularly important, we can define T^4 as a linear function. This gives us the ability to predict T^4 with high accuracy. We ignore higher-order variables as we proceed with the process of extending T^4 about the temperature of the free stream T using Taylor's series. A rough estimate may be found in the preceding, which can be obtained from this: The Rosseland mean absorption coefficient is expressed by the symbol k^* in this expression.

$$T^4\approx 4T_\infty^3-3T_\infty^4, \tag{9}$$

The equation for energy may be obtained by combining Eq. (8) and Eq. (9), as shown in the following

$$u\frac{\partial T}{\partial x}+v\frac{\partial T}{\partial y}=\frac{k}{\rho C_p}\frac{\partial^2 T}{\partial y^2}+\frac{Q_0}{\rho C_p}(T-T_\infty)+\tau\left(D_B\frac{\partial C}{\partial y}\frac{\partial T}{\partial y}+\frac{D_T}{T_\infty}\left(\frac{\partial T}{\partial y}\right)^2\right)+\frac{16\sigma^* T_\infty^3}{3\rho C_p k^*}\frac{\partial^2 T}{\partial y^2}, \tag{10}$$

Substitute Eq. (7) into Eq. (2), Eq. (3), Eq. (5) and Eq. (10) generate to acquire the succeeding non-dimensional equations.

$$\left(1+\frac{1}{\beta}\right)f'''+ff''-f'^2+Gr\theta+Gm\phi-\frac{M}{1+m^2}\left(f'+mg\right)=0 \tag{11}$$

$$\left(1+\frac{1}{\beta}\right)g''+fg'-f'g+\frac{M}{1+m^2}\left(mf'-g\right)=0 \tag{12}$$

$$\theta''(1+R\,\mathrm{Pr})+\mathrm{Pr}\,f\theta'+\mathrm{Pr}\,N_b\left(\theta'\phi'+\frac{N_T}{N_b}\theta'^2\right)+\mathrm{Pr}\,Q\theta=0 \tag{13}$$

$$\phi''+\mathrm{Pr}\ L_e\,f\,\phi'+\frac{N_t}{N_b}\theta''=0 \tag{14}$$

The dimensionless correlated boundary conditions (BCs) are as shadows

$$\begin{aligned} &f(0)=0,\quad f'(0)=1,\quad g(0)=0,\quad \theta(0)=0,\quad \phi(0)=1 \qquad at \quad \eta=0 \\ &f'(\eta)\to 0,\quad g(\eta)\to 0,\quad \theta(\eta)\to 0,\quad \phi(\eta)\to 0 \qquad as \quad \eta\to\infty \end{aligned} \tag{15}$$

The significant parameters are specified in the equations that do not include proportions

$$\begin{aligned} &M=\frac{\sigma B_0^2}{\rho a},\mathrm{Pr}=\frac{\nu}{\alpha}=\frac{\nu\rho C_p}{k},\ L_e=\frac{\alpha}{D_B},\ Q=\frac{Q_0}{a\rho C_p},Gr_x=\frac{g_c\beta_T(T_w-T_\infty)}{a^2x},\mathrm{Re}^2=\frac{ax^2}{\nu} \\ &N_b=\frac{\tau D_B(C_w-C_\infty)}{\nu},N_t=\frac{\tau D_T(T_w-T_\infty)}{\nu},Grc=\frac{g_c\beta_C(C_w-C_\infty)}{a^2x},R=\frac{16\sigma_1T_\infty^3}{3kk^*}. \end{aligned} \tag{16}$$

3. Physical Quantities of Interests

The relevant physical parameters that have an impact on the flow are the local skin friction coefficient in the direction of x Cf_x and the direction of z Cf_z, the local Nusselt number Nux, and the local Sherwood number Sh_x. The following explanations apply to these numerical values

$$C f_x=\frac{2\tau_{wx}}{\rho(ax)^2},\ Cf_z=\frac{2\tau_{wz}}{\rho(ax)^2},\ Nu_x=\frac{xq_w}{k(T_w-T_\infty)},\ Sh_x=\frac{x\,j_w}{D_B(C_w-C_\infty)} \tag{17}$$

where τwx, τwy, qw and jw are the wall skin friction, wall heat flux and wall mass flux respectively given by

$$\tau_{wx}=\mu\left[\frac{\partial u}{\partial y}\right]_{y=0},\quad \tau_{wz}=\mu\left[\frac{\partial w}{\partial y}\right]_{y=0},\ q_w=-k\left[\frac{\partial T}{\partial y}\right]_{y=0},\quad j_w=-D_B\left[\frac{\partial C}{\partial y}\right]_{y=0} \tag{18}$$

The following is an expression of the factor of skin friction, the Nusselt number, and the Sherwood number in their non-dimensional forms concerning the similarity component

$$\mathrm{Re}_x^{1/2}\,Cf_x=2f''(0),\quad \mathrm{Re}_x^{1/2}\,Cf_z=2g'(0),\ \mathrm{Re}_x^{1/2}\,Nu_x=-(1+R)\theta'(0),\ \mathrm{Re}_x^{1/2}\,Sh_x=-\phi'(0) \tag{19}$$

4. Results and Discussion

To envision the effect of various physical parameters on tangential velocity $f^i(\eta)$, transverse velocity g(η), nanoparticle concentration ϕ(η) and temperature θ(η) profiles, Figure 2 to 26 are plotted. In all these computations, unless mentioned, otherwise we have considered Nb= 0.3, Nt= 0.7, Pr= 0.71, Le = 0.6, β=0.5, M= 0.5, m= 0.2, Gr= 0.5, Gm = 0.5, Q=0.5, R=1

4.1 Effect of Magnetic Field Parameter (M)

Figure 2 to 5 show the effect of magnetic parameter M on the tangential velocity f ′(η), transverse velocity g(η), temperature θ(η), and concentration ϕ(η) profiles, respectively. The velocity profile f′(η) decreases with an increase in the values of M, the same behavior has observed transverse velocity g(η), and temperature θ(η) and concentration ϕ(η) profiles increase as M increases. As M increases, a drag force, called Lorentz force increases. Since this force opposes the flow of nanofluid, velocity in the flow direction decreases. Moreover, since an electrically conducting nanofluid with a strong magnetic field in the direction orthogonal to the flow is considered, an increase in M increases the force in the z-direction which results in a diminishes in the transverse velocity profile g(η).

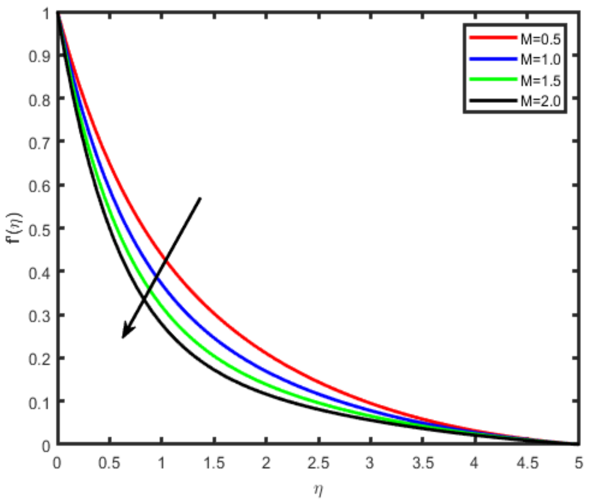

Fig. 2. Effect of M on f´(n)

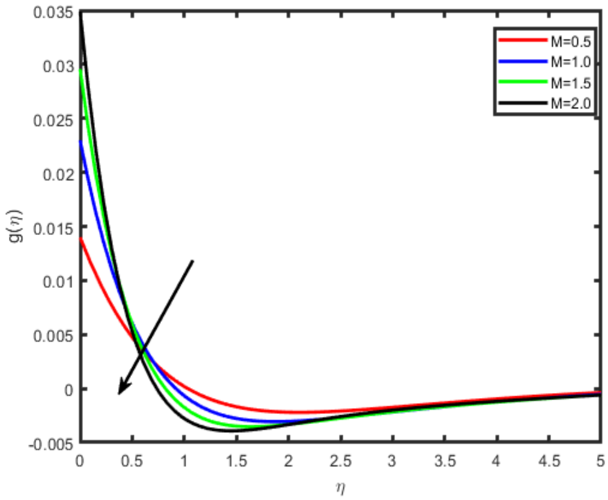

Fig. 3. Effect of M on g(n)

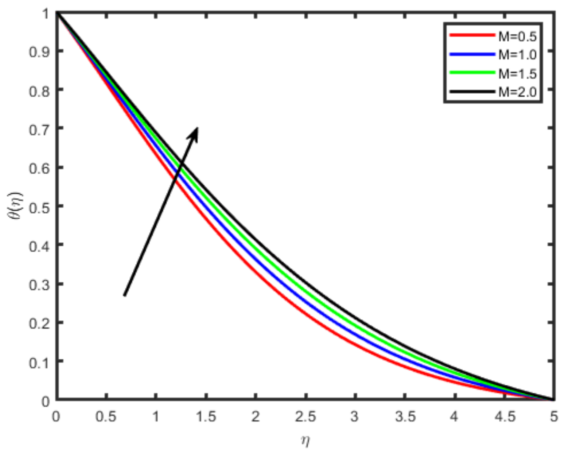

Fig. 4. Effect of M on θ(n)

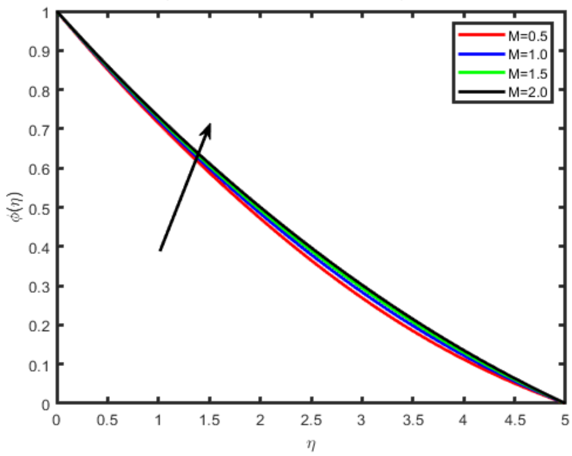

Fig. 5. Effect of M on φ (n)

4.2 Effect of Hall Current Parameter (M)

Figure 6 to 9 illustrate the impacts of the Hall parameter m on tangential velocity f'(η), transverse velocity g(η), nanoparticle concentration ϕ(η) and temperature θ(η) profiles, respectively. It is observed Figure 6 and 7, the velocity f'(η) and g(η) profiles increase as m increases. But, the temperature and concentration profiles decrease with an increase in m as shown in Figure 8 and 9. This is because the enclosure of Hall parameter decreases the resistive force caused by the magnetic field due to its effect of reducing the effective conductivity. Hence, the velocity component increases as the Hall parameter increases.

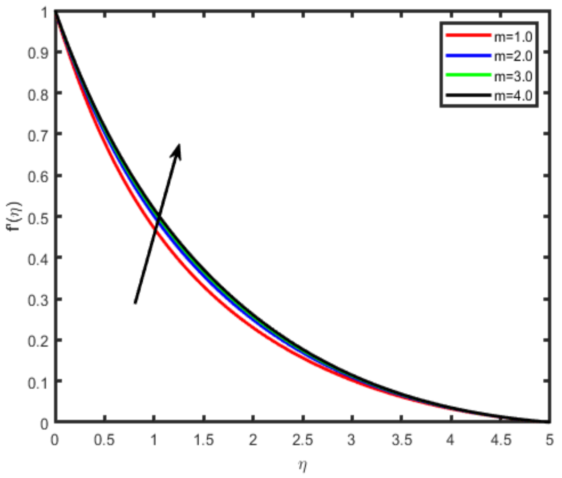

Fig. 6. Effect of m on f′(n)

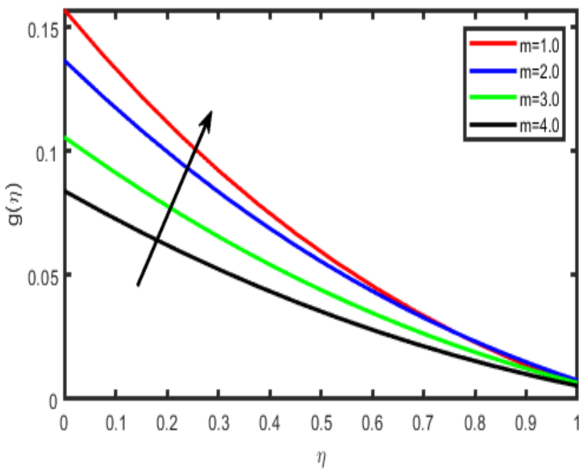

Fig. 7. Effect of m on g(n)

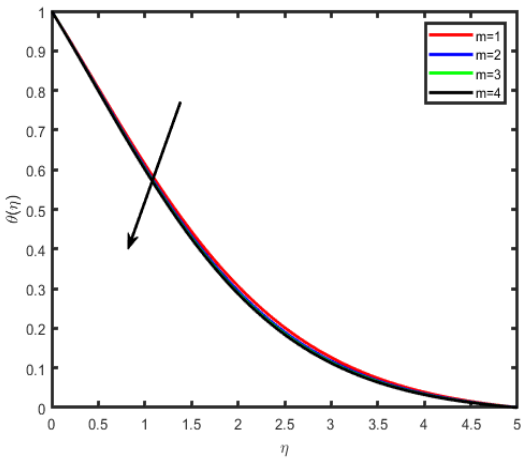

Fig. 8. Effect of m on θ(n)

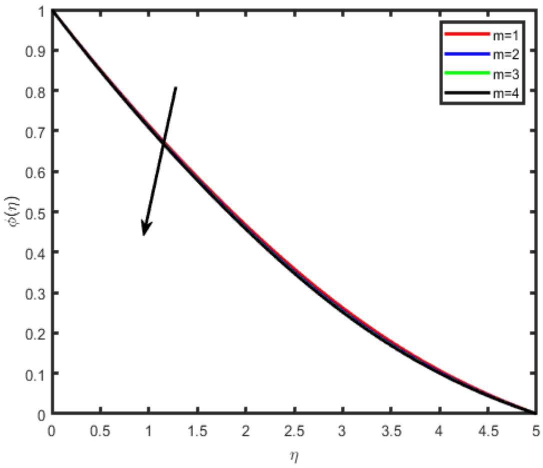

Fig. 9. Effect of m on φ (n)

4.3 Effect of Casson Fluid Parameter (B)

Figure 10 and 11 show the effect of the Casson parameter (β) on the velocity profiles. We notice that as β increases, the velocity and the boundary layer thickness decrease. Hence, the magnitude of the velocity is greater in Casson fluid when compared with viscous fluids.

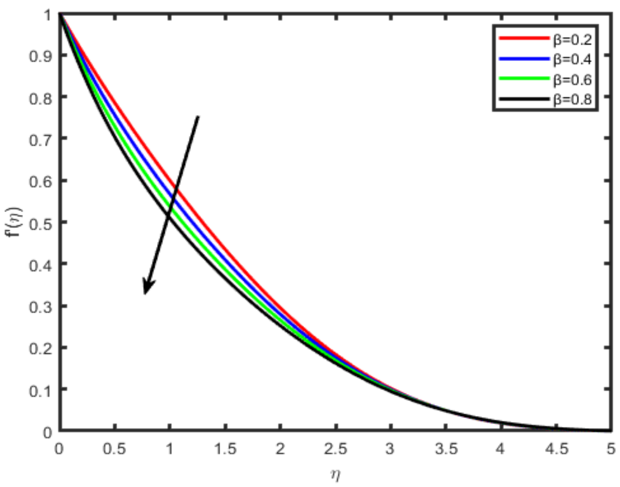

Fig. 10. Effect of β on f′(n)

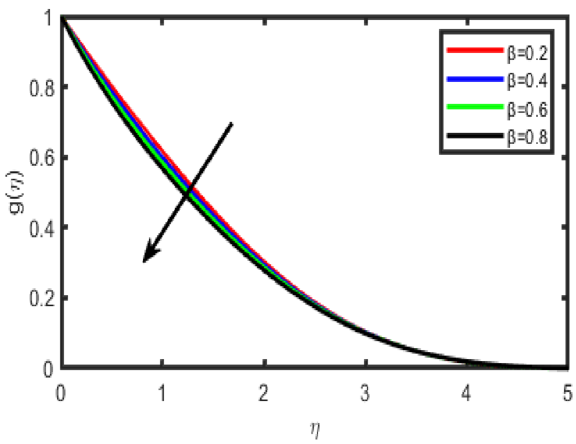

Fig. 11. Effect of β on g(n)

4.4 Effect of Thermal and Mass Grashof Numbers (Grx And Grc)

In Figure 12 to 15 the effects of the thermal Grashof Grx and mass Grashof Grc numbers on the tangential velocity $f''(\eta)$, the transverse velocity $g(\eta)$, are displayed respectively. As the Grashof number is a ratio of the buoyancy force to the viscous force and it appears due to the natural convection flow, so an increase in the tangential velocity as well as the transverse velocity of the fluid. It happens because of the fact that higher the Grashof number implies higher the buoyancy force which means higher the movement of the flow. Figure 8 and 9 depict the influence of the solutal Grashof number on the temperature and the concentration profile respectively. An increase in the solutal Grashof number means a decrease in the viscous force which reduces the temperature and the concentration of the fluid.

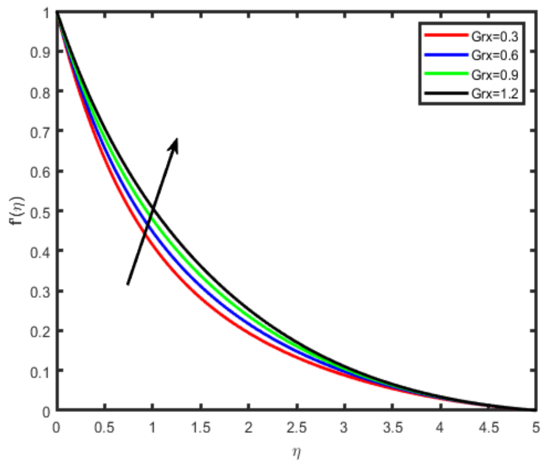

Fig. 12. Effect of Grx on f′(n)

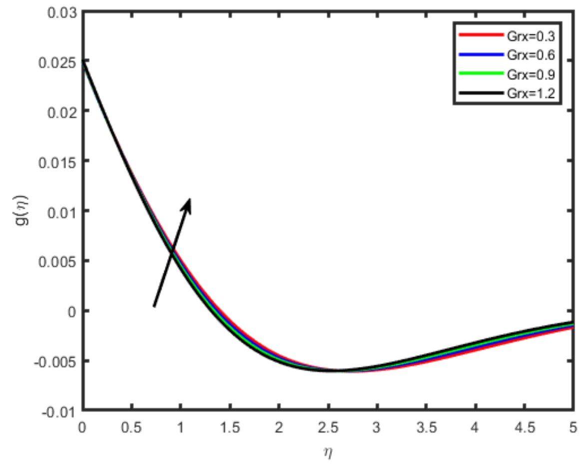

Fig. 13. Effect of Grx on g(n)

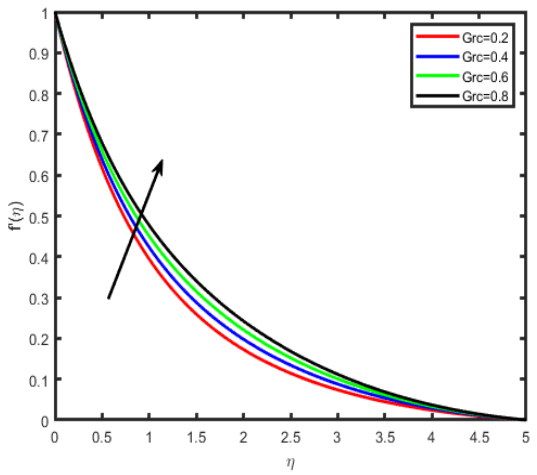

Fig. 14. Effect of Grc on f′(n)

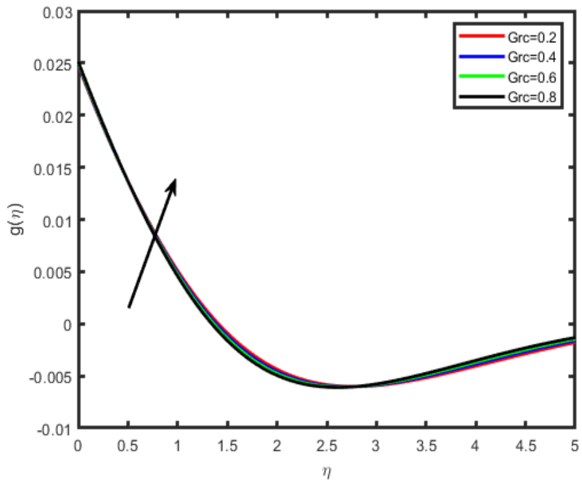

Fig. 15. Effect of Grc on g(n)

4.5 Effect of Radiation Parameter (R)

Figure 16 and 17 describes the behavior of thermal radiation parameter (R) on both temperature and concentration fields. It interesting to observe that for higher value of R strengthen the temperature because radiation parameter produces thermal energy in the flow region, therefore enhancement have been seen in the temperature field whereas reverse behavior is seen for concentration.

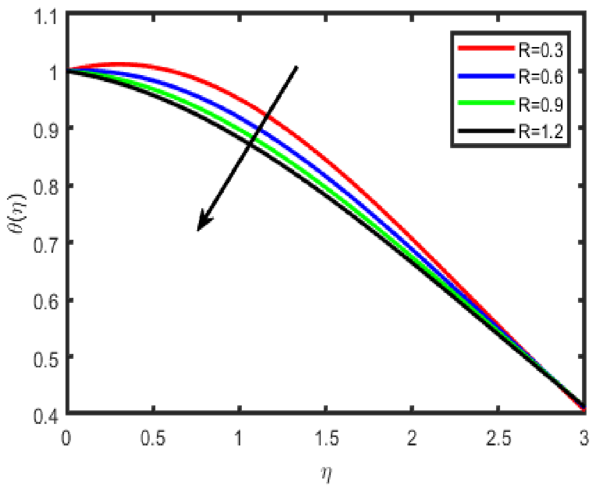

Fig. 16. Effect of R on θ(n)

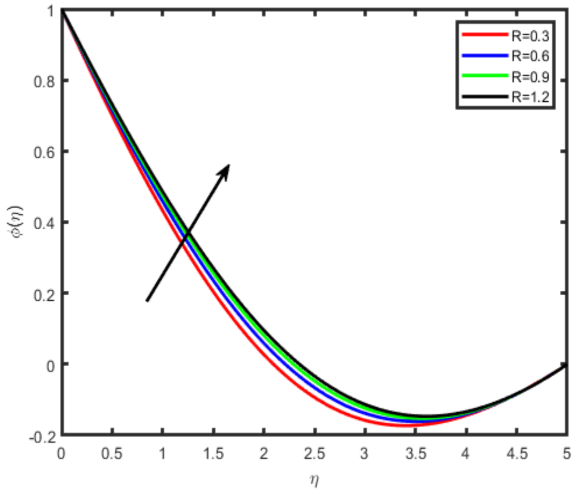

Fig. 17. Effect of R on φ(n)

4.6 Effect of Heat Source Parameter (Q)

Figure 18 shows that the temperature θ (η) increases with an increase in the resistance of the heat source/sink, due to an increase in the resistance of the heat generation, the temperature rises. The opposite behavior is observed in the case of concentration as expressed in Figure 19.

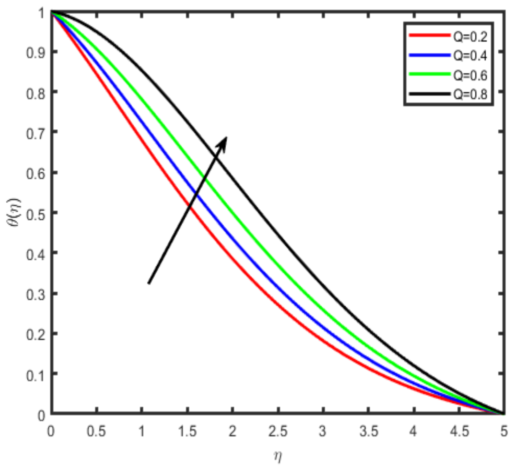

Fig. 18. Effect of Q on θ(n)

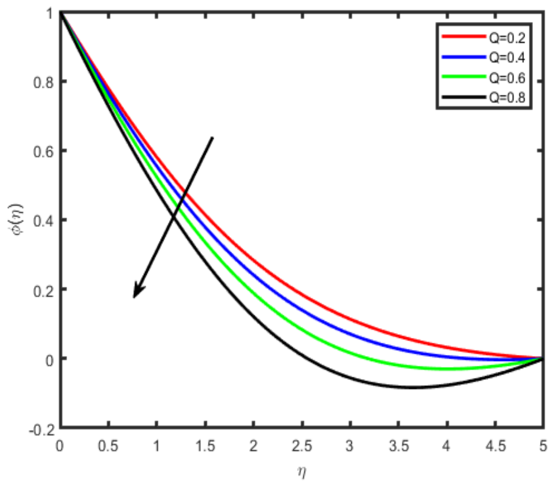

Fig. 19. Effect of Q on φ(n)

4.7 Effect of Brownian Motion Parameter (Nb)

The influence of Brownian motion parameter Nb on the temperature and concentration profiles is studied in Figure 20 and 21. From these figures, we notice that an enhancement in the values of Nb gives rise to the temperature, while it causes a decrease in the nanoparticle concentration profile. Brownian motion is the random motion of nanoparticles suspended in the fluid, caused by the collision of nanoparticles with the fluid particles. An increment in the thermophoretic effect causes an increment in the Brownian motion effect which results in the rise of the temperature due to the increment in the kinetic energy.

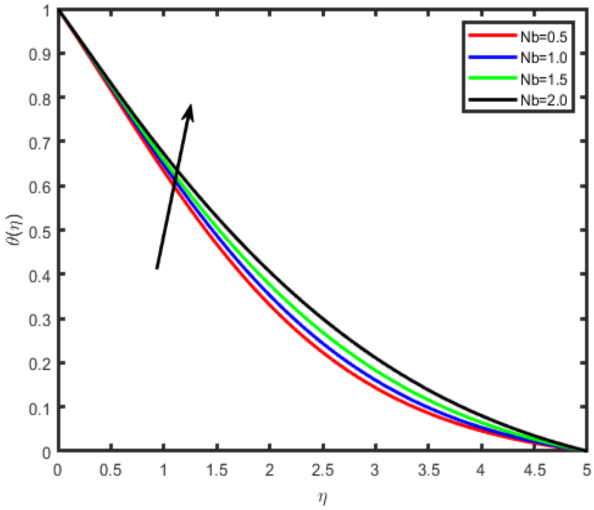

Fig. 20. Effect of Nb on θ(n)

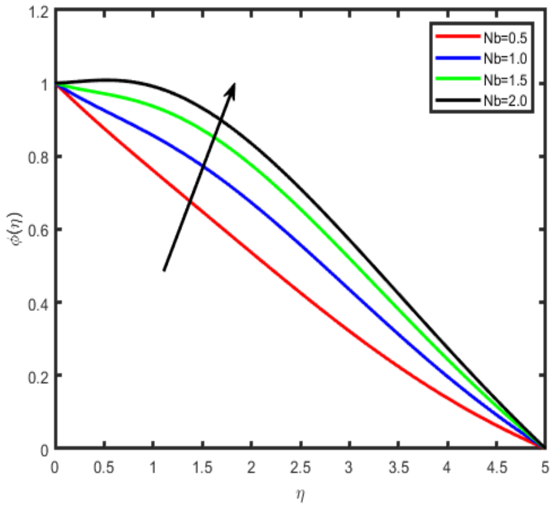

Fig. 21. Effect of Nb on φ(n)

4.8 Effect of Thermophoresis Parameter (Nt)

Figure 22 and 23 illustrate the effect of thermophoresis parameter Nt on the temperature and the nanoparticles concentration profile. One can observe that temperature and concentration fields increase with an enhancement in Nt. Thermophoresis parameter plays an important role in the heat transfer flow. Thermophoresis force enhances when Nt is increased which tends to move the nanoparticles from the hot region to the cold and as a result the temperature and the boundary layer thickness increase.

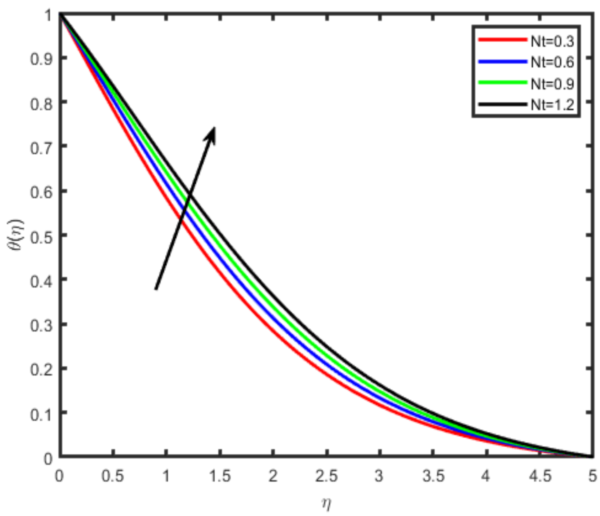

Fig. 22. Effect of Nt on θ(n)

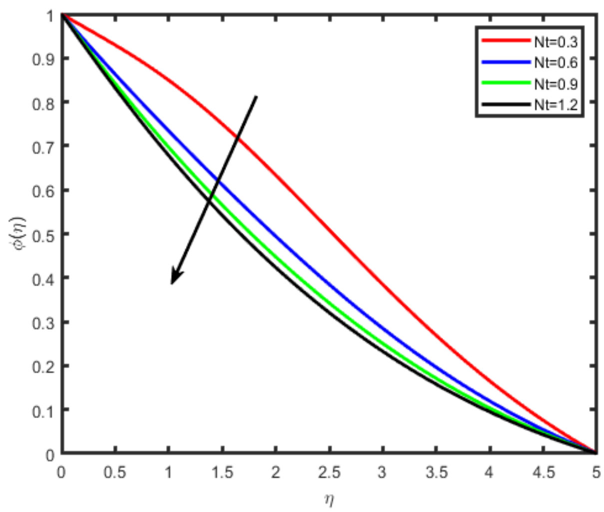

Fig. 23. Effect of Nt on φ(n)

4.9 Effect Lewis Number (Le)

Figure 24 and 25 show the impact of the Lewis number (Le) on temperature and nanoparticle concentration profiles respectively. It is observed that the temperature increases by increasing Le while concentration decreases with an increase in the Lewis number.

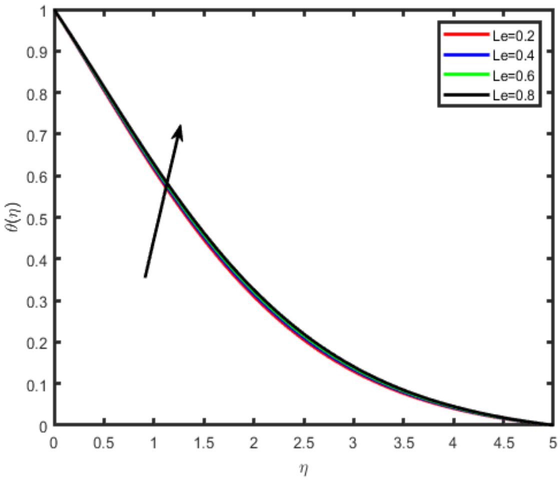

Fig. 24. Effect of Le on θ(n)

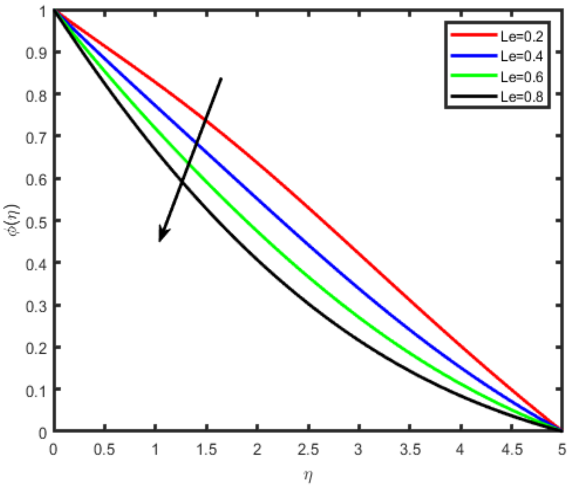

Fig. 25. Effect of Le on φ(n)

The impact of the various physical parameters on the local Sherwood number, skin friction coefficient and local Nusselt number, mathematical results are achieved for Nb= 0.3, β=0.5, Nt= 0.7, Pr= 0.71, Le = 0.6, M= 0.5, m= 0.2, Grx = 0.5, rc = 0.5, Q=0.5, and R=1are enumerated as shown in Table 1.

Table 1
Numerical values of $Re_x^{1/2}Cf_x, Re_x^{1/2}Cf_z, Re_x^{1/2}Nu_x, Re_x^{1/2}Sh_x$

Grx	Grc	Q	m	Nb	R	M	Pr	Nt	-2f''(0)	-2g'(0)	-θ'(0)	-ϕ'(0)
0.5									1.2547	0.8521	0.5212	0.9514
1.0									0.9978	0.9125	0.5323	0.9912
1.5									0.7354	0.9542	0.5457	1.0245
	0.3								0.9875	0.8512	0.5032	0.1247
	0.6								0.8475	0.9852	0.5124	0.1108
	0.9								0.7125	1.2521	0.5785	0.9178
			1						1.5214	0.8521	0.3145	0.8852
			2						1.0214	0.9547	0.2978	0.7952
			3						0.8125	0.9985	0.2312	0.9452
				0.2					0.9512	0.9521	0.8452	0.5852
				0.4					0.8152	0.9612	0.8215	0.6124
				0.6					0.7125	0.9852	0.8032	0.6978
						0.5			0.9452	1.0254	0.9875	0.7852
						1.0			1.2454	0.9852	0.9125	0.8952
						1.5			1.4035	0.8512	0.8952	0.9452
							0.68		0.9785	1.0214	0.1254	0.9878
							0.71		0.9120	0.9852	0.1578	0.9452
							0.76		0.8452	0.9032	0.1987	0.9231
								0.3	1.5452	0.9852	0.8542	0.5120
								0.6	1.1254	0.9120	0.8125	0.5921
								0.9	0.8752	0.8962	0.7521	0.6120
		0.2							0.7124	0.9875	0.9542	0.9852
		0.4							0.7852	0.9452	09125	0.9745
		06							0.8125	0.9132	0.8657	0.9645
					0.5				0.8752	1.0875	0.7452	0.9124
					1.0				0.8952	0.9442	0.7365	0.9120
					1.5				0.9125	0.9114	0.7154	0.9102

It is viewed that the skin-friction coefficient in x− direction decreases with an increase in the thermal Grashof number Grx, the mass Grashof number Grc, Hall current parameter m, and Brownian motion parameter Nb, while it increases for the increasing value of magnetic parameter M, Heat source parameter, Radiation and Prandtl number Pr, and thermophoresis parameter Nt. A completely opposite behavior is recorded for the coefficient of the skin-friction in the z-direction. Nusselt number increases when the Hall current parameter m, thermal Grashof number, the mass Grashof number, and Prandtl number, increase whereas it is reduced by increasing the value of Magnetic field parameter M, Heat source and radiation parameters. Sherwood number has increasing behavior for thermal Grashof number Gxr, Magnetic field parameter M, Brownian motion parameter Nb, Heat source and radiation parameters and thermophoresis parameter Nt, while it has decreasing behavior for Grashof number Grc and Prandtl number.

For the authentication of the numerical method used, the results were compared with the previously obtained results Sureshkumar *et al.,* [47] for various values of parameters and it indicates an excellent accord as shown in Table 2.

Table 2
Comparison of −θ′ (0) for various values of Pr when Nb= 0.3, Nt= 0.7, P r= 0.71, Le = 0.6, M= 0.5, Grx = 0.5, Grc= 0.5, m=0, Q=0, R=0, β=0

Pr	Suresh Kumar *et al.,* [47]	Present values
0.01	0.019125	0.01824563
0.72	0.807785	0.87937596
1	1.000000	1.00948958
3	1.924785	1.96-04968
10	3.732452	3.82049678

5. Conclusion

The conclusion that can be made from this research are

i. The resultant fluid velocity diminishes with increasing casson fluid parameter (β).
ii. The temperature increases as the Heat source/sink (Q) and Brownian motion parameter (Nb) values increase, but the concentration profile of nanoparticles decreases. The opposite behavior was observed for the case of Radiation parameter (R).
iii. The temperature and concentration fields intensify with a rise in the Thermophoresis parameter (Nt).
iv. The temperature increases by increasing Le while concentration decreases with an increase in the Lewis number
v. The velocity increases with enhance of hall parameter (m), where as the reversal behavior has observed in the case of temperature and Concentration.

Acknowledgement
This research was not funded by any grant.

References
[1] Rathod, V. P., and Shakera Tanveer. "Pulsatile flow of couple stress fluid through a porous medium with periodic body acceleration and magnetic field." *Bulletin of the Malaysian Mathematical Sciences Society* 32, no. 2 (2009).
[2] Krishnan, B. CHANDRAN, S. E. Rittgers, and A. P. Yoganathan. "Biouid Mechanics: The Human Circulation." (2012). https://doi.org/10.1201/b11709

[3] Blair, GW Scott. "An equation for the flow of blood, plasma and serum through glass capillaries." *Nature* 183 (1959): 613-614. https://doi.org/10.1038/183613a0
[4] Casson, N. "Flow equation for pigment-oil suspensions of the printing ink-type." *Rheology of disperse systems* (1959): 84-104.
[5] Li, Shuguang, Kodi Raghunath, Ayman Alfaleh, Farhan Ali, A. Zaib, M. Ijaz Khan, Sayed M. ElDin, and V. Puneeth. "Effects of activation energy and chemical reaction on unsteady MHD dissipative Darcy–Forchheimer squeezed flow of Casson fluid over horizontal channel." *Scientific Reports* 13, no. 1 (2023): 2666. https://doi.org/10.1038/s41598-023-29702-w
[6] Suresh Kumar, Y., Shaik Hussain, K. Raghunath, Farhan Ali, Kamel Guedri, Sayed M. Eldin, and M. Ijaz Khan. "Numerical analysis of magnetohydrodynamics Casson nanofluid flow with activation energy, Hall current and thermal radiation." *Scientific Reports* 13, no. 1 (2023): 4021. https://doi.org/10.1038/s41598-023-28379-5
[7] Khan, Umair, Fateh Mebarek-Oudina, Aurang Zaib, Anuar Ishak, Sakhinah Abu Bakar, El-Sayed M. Sherif, and Dumitru Baleanu. "An exact solution of a Casson fluid flow induced by dust particles with hybrid nanofluid over a stretching sheet subject to Lorentz forces." *Waves in Random and Complex Media* (2022): 1-14. https://doi.org/10.1080/17455030.2022.2102689
[8] Raza, J., F. Mebarek-Oudina, and L. Ali Lund. "The flow of magnetised convective Casson liquid via a porous channel with shrinking and stationary walls." *Pramana* 96, no. 4 (2022): 229. https://doi.org/10.1007/s12043-022-02465-1
[9] Sohail, Muhammad, Yu-Ming Chu, Essam R. El-Zahar, Umar Nazir, and Tahir Naseem. "Contribution of joule heating and viscous dissipation on three dimensional flow of Casson model comprising temperature dependent conductance utilizing shooting method." *Physica Scripta* 96, no. 8 (2021): 085208. https://doi.org/10.1088/1402-4896/ac00e5
[10] Mebarek-Oudina, F., Preeti, A. S. Sabu, H. Vaidya, R. W. Lewis, S. Areekara, A. Mathew, and A. I. Ismail. "Hydromagnetic flow of magnetite–water nanofluid utilizing adapted Buongiorno model." *International Journal of Modern Physics B* (2023): 2450003. https://doi.org/10.1142/S0217979224500036
[11] Kodi, Raghunath, and Obulesu Mopuri. "Unsteady MHD oscillatory Casson fluid flow past an inclined vertical porous plate in the presence of chemical reaction with heat absorption and Soret effects." *Heat Transfer* 51, no. 1 (2022): 733-752. https://doi.org/10.1002/htj.22327
[12] Kodi, Raghunath, Obulesu Mopuri, Sujatha Sree, and Venkateswaraju Konduru. "Investigation of MHD Casson fluid flow past a vertical porous plate under the influence of thermal diffusion and chemical reaction." *Heat Transfer* 51, no. 1 (2022): 377-394. https://doi.org/10.1002/htj.22311
[13] Choi, S. US, and Jeffrey A. Eastman. *Enhancing thermal conductivity of fluids with nanoparticles*. No. ANL/MSD/CP-84938; CONF-951135-29. Argonne National Lab.(ANL), Argonne, IL (United States), 1995.
[14] Murshed, S. M. S., K. C. Leong, and C. Yang. "Thermophysical and electrokinetic properties of nanofluids–a critical review." *Applied thermal engineering* 28, no. 17-18 (2008): 2109-2125. https://doi.org/10.1016/j.applthermaleng.2008.01.005
[15] Özerinç, Sezer, Sadık Kakaç, and Almıla Güvenç Yazıcıoğlu. "Enhanced thermal conductivity of nanofluids: a state-of-the-art review." *Microfluidics and Nanofluidics* 8 (2010): 145-170. https://doi.org/10.1007/s10404-009-0524-4
[16] Wong, Kaufui V., and Omar De Leon. "Applications of nanofluids: current and future." *Advances in mechanical engineering* 2 (2010): 519659. https://doi.org/10.1155/2010/519659
[17] Buongiorno, Jacopo. "Convective transport in nanofluids." (2006): 240-250. https://doi.org/10.1115/1.2150834
[18] Mebarek-Oudina, Fateh. "Convective heat transfer of Titania nanofluids of different base fluids in cylindrical annulus with discrete heat source." *Heat Transfer—Asian Research* 48, no. 1 (2019): 135-147. https://doi.org/10.1002/htj.21375
[19] Shafiq, Anum, Fateh Mebarek-Oudina, T. N. Sindhu, and G. Rasool. "Sensitivity analysis for Walters-B nanoliquid flow over a radiative Riga surface by RSM." *Scientia Iranica* 29, no. 3 (2022): 1236-1249.
[20] Mebarek-Oudina, F., and I. Chabani. "Review on nano-fluids applications and heat transfer enhancement techniques in different enclosures." *Journal of Nanofluids* 11, no. 2 (2022): 155-168. https://doi.org/10.1166/jon.2022.1834
[21] Dharmaiah, G., Fateh Mebarek-Oudina, M. Sreenivasa Kumar, and K. Chandra Kala. "Nuclear reactor application on Jeffrey fluid flow with Falkner-skan factor, Brownian and thermophoresis, non linear thermal radiation impacts past a wedge." *Journal of the Indian Chemical Society* 100, no. 2 (2023): 100907. https://doi.org/10.1016/j.jics.2023.100907
[22] Chabani, I., F. Mebarek-Oudina, H. Vaidya, and A. I. Ismail. "Numerical analysis of magnetic hybrid Nano-fluid natural convective flow in an adjusted porous trapezoidal enclosure." *Journal of Magnetism and Magnetic Materials* 564 (2022): 170142. https://doi.org/10.1016/j.jmmm.2022.170142

[23] Umair, Muhammad, Daeun Kim, and Minha Choi. "Impact of climate, rising atmospheric carbon dioxide, and other environmental factors on water-use efficiency at multiple land cover types." *Scientific Reports* 10, no. 1 (2020): 1-13. https://doi.org/10.1038/s41598-020-68472-7

[24] Raza, Rabeeah, Muhammad Sohail, Thabet Abdeljawad, Rahila Naz, and Phatiphat Thounthong. "Exploration of temperature-dependent thermal conductivity and diffusion coefficient for thermal and mass transportation in sutterby nanofluid model over a stretching cylinder." *Complexity* 2021 (2021): 1-14. https://doi.org/10.1155/2021/6252864

[25] Sohail, Muhammad, Umar Nazir, Yu-Ming Chu, Hussam Alrabaiah, Wael Al-Kouz, and Phatiphat Thounthong. "Computational exploration for radiative flow of Sutterby nanofluid with variable temperature-dependent thermal conductivity and diffusion coefficient." *Open Physics* 18, no. 1 (2020): 1073-1083. https://doi.org/10.1515/phys-2020-0216

[26] Naseem, Tahir, Umar Nazir, and Muhammad Sohail. "Contribution of Dufour and Soret effects on hydromagnetized material comprising temperature-dependent thermal conductivity." *Heat Transfer* 50, no. 7 (2021): 7157-7175. https://doi.org/10.1002/htj.22222

[27] Wang, Fuzhang, Umar Nazir, Muhammad Sohail, Essam R. El-Zahar, Choonkil Park, and Phatiphat Thounthong. "A Galerkin strategy for tri-hybridized mixture in ethylene glycol comprising variable diffusion and thermal conductivity using non-Fourier's theory." *Nanotechnology Reviews* 11, no. 1 (2022): 834-845. https://doi.org/10.1515/ntrev-2022-0050

[28] Algehyne, Ebrahem A., Essam R. El-Zahar, S. H. Elhag, Fatimah S. Bayones, Umar Nazir, Muhammad Sohail, and Poom Kumam. "Investigation of thermal performance of Maxwell hybrid nanofluid boundary value problem in vertical porous surface via finite element approach." *Scientific Reports* 12, no. 1 (2022): 2335. https://doi.org/10.1038/s41598-022-06213-8

[29] Sohail, Muhammad, Umair Ali, Qasem Al-Mdallal, Phatiphat Thounthong, El-Sayed M. Sherif, Hussam Alrabaiah, and Zahra Abdelmalek. "Theoretical and numerical investigation of entropy for the variable thermophysical characteristics of couple stress material: Applications to optimization." *Alexandria Engineering Journal* 59, no. 6 (2020): 4365-4375. https://doi.org/10.1016/j.aej.2020.07.042

[30] Maatoug, Samah, K. Hari Babu, V. V. L. Deepthi, Kaouther Ghachem, Kodi Raghunath, Charankumar Ganteda, and Sami Ullah Khan. "Variable chemical species and thermo-diffusion Darcy–Forchheimer squeezed flow of Jeffrey nanofluid in horizontal channel with viscous dissipation effects." *Journal of the Indian Chemical Society* 100, no. 1 (2023): 100831. https://doi.org/10.1016/j.jics.2022.100831

[31] Bafakeeh, Omar T., Kodi Raghunath, Farhan Ali, Muhammad Khalid, El Sayed Mohamed Tag-ElDin, Mowffaq Oreijah, Kamel Guedri, Nidhal Ben Khedher, and Muhammad Ijaz Khan. "Hall current and Soret effects on unsteady MHD rotating flow of second-grade fluid through porous media under the influences of thermal radiation and chemical reactions." *Catalysts* 12, no. 10 (2022): 1233. https://doi.org/10.3390/catal12101233

[32] Deepthi, V. V. L., Maha MA Lashin, N. Ravi Kumar, Kodi Raghunath, Farhan Ali, Mowffaq Oreijah, Kamel Guedri, El Sayed Mohamed Tag-ElDin, M. Ijaz Khan, and Ahmed M. Galal. "Recent development of heat and mass transport in the presence of Hall, ion slip and thermo diffusion in radiative second grade material: application of micromachines." *Micromachines* 13, no. 10 (2022): 1566. https://doi.org/10.3390/mi13101566

[33] Ganjikunta, Aruna, Hari Babu Kommaddi, Venkateswarlu Bhajanthri, and Raghunath Kodi. "An unsteady MHD flow of a second-grade fluid passing through a porous medium in the presence of radiation absorption exhibits Hall and ion slip effects." *Heat Transfer* (2023). https://doi.org/10.1002/htj.22716

[34] Md. Rafiqul Islam, Md. Asaduzzaman, Md. Mahmud Alam, "Hall current effects on one dimensional unsteady MHD micropolar fluid flow past an impulsive started plate", *International Journal of Engineering Technology Science and Research* 2, (2015): 79–88.

[35] Kodi, Raghunath, Mohanaramana Ravuri, Nagesh Gulle, Charankumar Ganteda, Sami Ullah Khan, and M. Ijaz Khan. "Hall and ion slip radiative flow of chemically reactive second grade through porous saturated space via perturbation approach." *Waves in Random and Complex Media* (2022): 1-17. https://doi.org/10.1080/17455030.2022.2108555

[36] Raghunath, Kodi, G. Charankumar, and L. Giulio. "Effects of Soret, rotation, Hall, and ion slip on unsteady MHD flow of a Jeffrey fluid through a porous medium in the presence of heat absorption and chemical reaction." *J. Mech. Eng. Res. Dev* 45, no. 3 (2022): 80-97.

[37] Raghunath, Kodi, and Ravuri Mohanaramana. "Hall, Soret, and rotational effects on unsteady MHD rotating flow of a second-grade fluid through a porous medium in the presence of chemical reaction and aligned magnetic field." *International Communications in Heat and Mass Transfer* 137 (2022): 106287. https://doi.org/10.1016/j.icheatmasstransfer.2022.106287

[38] Reddy, Yanala Dharmendar, Dodda Ramya, and Laxmianarayanagari Anand Babu. "Effect of thermal radiation on MHD boundary layer flow of nanofluid and heat transfer over a non-linearly stretching sheet with transpiration." *Journal of Nanofluids* 5, no. 6 (2016): 889-897. https://doi.org/10.1166/jon.2016.1284

[39] Kothandapani, M., and J. Prakash. "Effects of thermal radiation parameter and magnetic field on the peristaltic motion of Williamson nanofluids in a tapered asymmetric channel." *International Journal of Heat and Mass Transfer* 81 (2015): 234-245. https://doi.org/10.1016/j.ijheatmasstransfer.2014.09.062

[40] Sulochana, C., S. Payad Samrat, and N. Sandeep. "Thermal radiation effect on MHD nanofluid flow over a stretching sheet." In *International Journal of Engineering Research in Africa*, vol. 23, pp. 89-102. Trans Tech Publications Ltd, 2016. https://doi.org/10.4028/www.scientific.net/JERA.23.89

[41] Kho, Yap Bing, Abid Hussanan, Norhafizah Mohd Sarif, Zulkhibri Ismail, and Mohd Zuki Salleh. "Thermal radiation effects on MHD with flow heat and mass transfer in Casson nanofluid over a stretching sheet." In *MATEC Web of Conferences*, vol. 150, p. 06036. EDP Sciences, 2018. https://doi.org/10.1051/matecconf/201815006036

[42] Zubair, Tamour, Muhammad Usman, Muhammad Hamid, Muhammad Sohail, Umar Nazir, Kottakkaran Sooppy Nisar, and Velusamy Vijayakumar. "Computational analysis of radiative Williamson hybrid nanofluid comprising variable thermal conductivity." *Japanese Journal of Applied Physics* 60, no. 8 (2021): 087004. https://doi.org/10.35848/1347-4065/ac1388

[43] Raghunath, Kodi, Nagesh Gulle, Ramachandra Reddy Vaddemani, and Obulesu Mopuri. "Unsteady MHD fluid flow past an inclined vertical porous plate in the presence of chemical reaction with aligned magnetic field, radiation, and Soret effects." *Heat Transfer* 51, no. 3 (2022): 2742-2760. https://doi.org/10.1002/htj.22423

[44] Kodi, Raghunath, and Mohana Ramana Ravuri. "Soret and Chemical Reaction Effects on Heat and Mass Transfer in MHD Flow of a Kuvshinski Fluid Through Porous Medium with Aligned Magnetic Field and Radiation." In *Nonlinear Dynamics and Applications: Proceedings of the ICNDA 2022*, pp. 377-391. Cham: Springer International Publishing, 2022. https://doi.org/10.1007/978-3-030-99792-2_32

[45] Mohana Ramana, R., K. Venkateswara Raju, and K. Raghunath. "Chemical reaction with aligned magnetic field effects on unsteady MHD Kuvshinski fluid flow past an inclined porous plate in the presence of radiation and Soret effects." *Heat Transfer* 51, no. 7 (2022): 6431-6449. https://doi.org/10.1002/htj.22598

[46] Mopuri, Obulesu, Raghunath Kodi, Charankumar Ganteda, Ramu Srikakulapu, and Giulio Lorenzini. "MHD heat and mass transfer steady flow of a convective fluid through a porous plate in the presence of diffusion thermo and aligned magnetic field." *Journal of Advanced Research in Fluid Mechanics and Thermal Sciences* 89, no. 1 (2022): 62-76. https://doi.org/10.37934/arfmts.89.1.6276

[47] Suresh Kumar, Y., Shaik Hussain, K. Raghunath, Farhan Ali, Kamel Guedri, Sayed M. Eldin, and M. Ijaz Khan. "Numerical analysis of magnetohydrodynamics Casson nanofluid flow with activation energy, Hall current and thermal radiation." *Scientific Reports* 13, no. 1 (2023): 4021. https://doi.org/10.1038/s41598-023-28379-5

[48] Sutton, George W., and Arthur Sherman. *Engineering magnetohydrodynamics*. McGraw-Hill, New York. USA, 1965.

[49] Abo-Eldahab, Emad M., and Mohamed A. El Aziz. "Hall and ion-slip effects on MHD free convective heat generating flow past a semi-infinite vertical flat plate." *Physica Scripta* 61, no. 3 (2000): 344. https://doi.org/10.1238/Physica.Regular.061a00344